7-2013

HfCo7-Based Rare-Earth-Free Permanent-Magnet Alloys

Bhaskar Das
University of Nebraska-Lincoln, bhaskar.das@huskers.unl.edu

Balamurugan Balamurugan
University of Nebraska-Lincoln, balamurugan@unl.edu

Pankaj Kumar
Kendriya Vidhyalaya, panksamrat@gmail.com

Ralph Skomski
University of Nebraska-Lincoln, rskomski2@unl.edu

Shah R. Valloppilly
University of Nebraska-Lincoln, svalloppilly2@unl.edu

See next page for additional authors

$HfCo_7$-Based Rare-Earth-Free Permanent-Magnet Alloys

B. Das[1,2], B. Balamurugan[1,2], Pankaj Kumar[3], R. Skomski[1,2], V. R. Shah[1], J. E. Shield[1,4], A. Kashyap[3], and D. J. Sellmyer[1,2]

[1]Nebraska Center for Materials and Nanoscience, University of Nebraska, Lincoln, NE 68588 USA
[2]Department of Physics and Astronomy, University of Nebraska, Lincoln, NE 68588 USA
[3]School of Basic Sciences, Indian Institute of Technology, Mandi 175 001, India
[4]Department of Mechanical and Materials Engineering, University of Nebraska, Lincoln, NE 68588 USA

This study presents the structural and magnetic properties of melt-spun $HfCo_7$, $HfCo_{7-x}Fe_x$ $(0.25 \leq x \leq 1)$, and $HfCo_7Si_x$ $(0.2 \leq x \leq 1.2)$ alloys. Appreciable permanent-magnet properties with a magnetocrystalline anisotropy of about 9.6–16.5 $\mathrm{Mergs/cm^3}$, a magnetic polarization $J_s \approx 7.2$–10.6 kG, and coercivities $H_c = 0.5$–3.0 kOe were obtained by varying the composition of these alloys. Structural analysis reveals that the positions of x-ray diffraction peaks of $HfCo_7$ show good agreement with those corresponding to an orthorhombic structure having lattice parameters of about $a = 4.719$ Å, $b = 4.278$ Å, and $c = 8.070$ Å. Based on these results, a model crystal structure for $HfCo_7$ is developed and used to estimate the magnetic properties of $HfCo_7$ using density-functional calculations, which agree with the experimental results.

***Index Terms*—Doping, magnetocrystalline anisotropy, permanent magnets, rare-earth-free alloys.**

I. Introduction

RECENTLY, the search for rare-earth-free alloys with magnetocrystalline anisotropy $K_1 \geq 10\ \mathrm{Mergs/cm^3}$ and magnetic polarization $J_s \geq 10$ kG ($J_s = 4\pi M_s$, M_s is saturation magnetization) has become the thrust area of permanent-magnet research, which is aimed at satisfying the rapidly growing demand for rare-earth elements and reducing the cost of the permanent magnets for bulk applications [1]–[3]. In this regard, the $HfCo_7$ intermetallic phase has shown high Curie temperature T_c (~600 K) and J_s (~10 kG), and is reported to form a non-cubic crystal structure, which can cause a high K_1 suitable for permanent-magnet applications [4]–[8]. However, according to Co-Hf binary phase diagram, the $HfCo_7$ phase forms only at a single composition (12.5 at. % of Hf) and temperatures above 1000°C under thermal equilibrium conditions [9]; thus it is challenging to control the phase purity and crystal structure, which is important to obtain permanent-magnet properties in $HfCo_7$. These limitations presumably restricted earlier studies on bulk $HfCo_7$ alloys, which do not provide a detailed structural analysis and other vital information such as magnetic anisotropies and coercivities [4]–[8].

In particular, the crystal structure of $HfCo_7$ is insufficiently known, with conflicting reports on unit cells (tetragonal, hexagonal or orthorhombic) and without information about individual atomic positions [4]–[7]. Recently, stoichiometric $HfCo_7$ nanoparticles were produced using a gas-aggregation-type cluster-deposition system. These nanoparticles have shown permanent-magnet properties with a $K_1 \approx 10\ \mathrm{Mergs/cm^3}$ and $H_c \approx 4.4$ kOe at 300 K and their x-ray diffraction peaks could be indexed with an orthorhombic structure [10]. In the present study, we have investigated the structural and magnetic properties of melt-spun $HfCo_7$, $HfCo_{7-x}Fe_x$ and $HfCo_7Si_x$ bulk alloys, and also proposed a model crystal structure for $HfCo_7$, which provides an opportunity to estimate the magnetic properties using density-functional calculations and new insights in understanding the underlying magnetic properties of $HfCo_7$-based alloys. Note that the rapid cooling during the melt-spinning process is advantageous in obtaining the phase purity and desired crystal structure in these alloys.

Manuscript received October 23, 2012; revised January 14, 2013; accepted January 16, 2013. Date of current version July 15, 2013. Corresponding author: B. Balamurugan (e-mail: bbalasubramanian2@unl.edu).

Color versions of one or more of the figures in this paper are available online at http://ieeexplore.ieee.org.

Digital Object Identifier 10.1109/TMAG.2013.2242856

II. Experimental and Theoretical Methods

Ribbons of $HfCo_7$, $HfCo_{7-x}Fe_x$ $(0.25 \leq x \leq 1)$, and $HfCo_7Si_x$ $(0.2 \leq x \leq 1.2)$ were fabricated by melt spinning. For this, alloys with the above-mentioned nominal compositions were made from high purity (>99.95%) elements using conventional arc melting followed by melt spinning in high-purity argon atmosphere at a tangential wheel velocity of 40 m/s. Bulk ribbons were characterized using a superconducting quantum interference device (SQUID) magnetometer, energy dispersive x-ray spectroscopy (EDX, JEOL JSM 840A scanning electron microscope), and x-ray diffractometer (XRD, Rigaku D/Max-B diffractometer).

For model calculations, we use frozen-core full-potential projector-augmented-wave method as implemented in the Vienna *Ab-Initio* Simulation Package (VASP) within the framework of density-functional theory (DFT) [11], [12]. The exchange and correlation effects are described by the method of Perdew, Burke and Ernzerhof using the generalized-gradient approximation (GGA) [13].

III. Experimental Results

XRD patterns for $HfCo_7$, $HfCo_{6.5}Fe_{0.5}$, and $HfCo_7Si_{0.4}$ are shown in Fig. 1. We have carried out the peak indexing analysis on the XRD pattern of $HfCo_7$ (curve i in Fig. 1) using TOPAS (Total Pattern Analysis Solution, Bruker AXS) by assuming all the reported crystal structures such as hexagonal, tetragonal or orthorhombic. The positions of the experimental XRD peaks of $HfCo_7$ (curve i Fig. 1) show good agreement with the diffraction-peak positions determined using TOPAS (vertical lines in Fig. 1(a)) for an orthorhombic structure having lattice parameters of about $a = 4.719$ Å, $b = 4.278$ Å, and $c = 8.070$ Å.

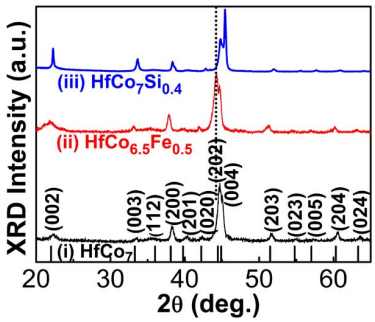

Fig. 1. X-ray diffraction patterns for $HfCo_7$, $HfCo_{6.5}Fe_{0.5}$, and $HfCo_7Si_{0.4}$, where the XRD peak positions determined using TOPAS for orthorhombic structure are shown as vertical lines. A shift in the XRD peak positions of $HfCo_{6.5}Fe_{0.5}$ as compared to those of $HfCo_7$ is guided by a vertical dotted line.

Fig. 1 also reveals that $HfCo_{7-x}Fe_x$ and $HfCo_7Si_x$ alloys have XRD patterns similar to $HfCo_7$ (curve i) as shown in the case of $HfCo_{6.5}Fe_{0.5}$ (curve ii) and $HfCo_7Si_{0.4}$ (curve iii). In addition, $HfCo_{6.5}Fe_{0.5}$ exhibits a shift in the angular position of the diffraction peaks towards lower angle side (for example, as indicated by a dotted line in the case of (202) peak of $HfCo_{6.5}Fe_{0.5}$) as compared to $HfCo_7$ and this result reveals a lattice expansion on the substitution of Fe for Co in $HfCo_{7-x}Fe_x$. In the case of $HfCo_7Si_{0.4}$, the position of XRD peaks does not show considerable shift with respect to that of $HfCo_7$, presumably due to the interstitial occupation of Si in $HfCo_7$ lattice. Interestingly, alloying of $HfCo_7$ with Si improves the crystallinity of these alloys as revealed by the sharp diffraction peaks in the case of $HfCo_7Si_{0.4}$, as compared to $HfCo_7$ and $HfCo_{6.5}Fe_{0.5}$.

The magnetic properties of the $HfCo_7$, $HfCo_{7-x}Fe_x$, and $HfCo_7Si_x$ alloys were investigated by measuring the magnetization (M) curves at 300 K as a function of applied magnetic field H from -70 to 70 kOe and show two important features. First, the expanded room-temperature $M-H$ curves from $H=-25$ to 25 kOe for $HfCo_7$, $HfCo_{6.5}Fe_{0.5}$, and $HfCo_7Si_{0.4}$ show high H_c as shown in Fig. 2(a), as compared to $H_c \approx 0.09$ kOe for bulk hcp Co (not shown in Fig. 2(a)). Second, M does not attain complete saturation even at $H = 70$ kOe as shown by the $M-H$ curves in the high-field region (Fig. 2(b)) and this behavior indicates a large value of magnetic anisotropy in $HfCo_7$-based alloys. The magnetic anisotropy constant K_1 was estimated from the high field region of the experimental $M-H$ curves ($H > 30$ kOe) using the law of approach to saturation method, widely used for randomly oriented magnets [14]–[16].

$$M = M_s\left(1-\frac{A}{H^2}\right)+\chi H \tag{1}$$

In (1), χ is the high-field susceptibility and the constant A depends on the anisotropy constant K_1 as given by

$$A = \frac{4}{15}\frac{K_1^2}{M_s^2} \tag{2}$$

The experimental M (solid spheres) in the high field region ($H > 30$ kOe) is fitted as represented by solid lines using (1) to estimate K_1 as shown in Fig. 2(b). This evaluation reveals high magnetic anisotropies of about 10 $\mathrm{Mergs/cm^3}$ in

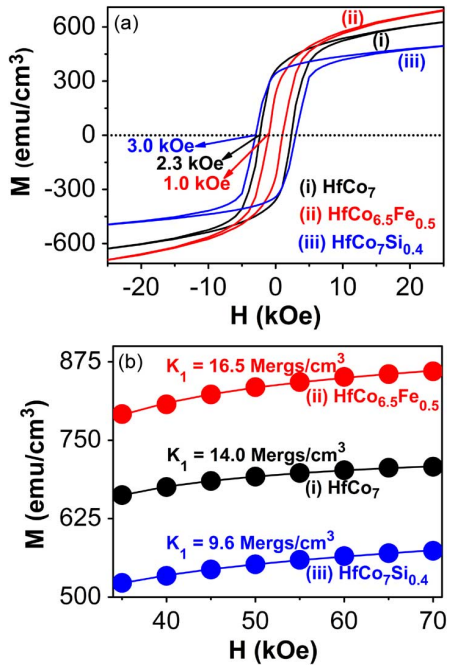

Fig. 2. (a) The expanded $M-H$ curves from $H=-25$ to 25 kOe for $HfCo_7$, $HfCo_{6.5}Fe_{0.5}$, and $HfCo_7Si_{0.4}$ alloys measured at 300 K (b) An estimation of magnetic anisotropy constant K_1 from the high-field region of room-temperature M vs. H curves ($H > 30$ kOe) using the law of approach to saturation method [14]–[16]. The solid spheres and lines represent the corresponding experimental data and fittings, respectively.

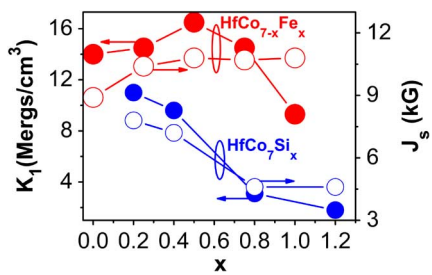

Fig. 3. The measured values of magnetic anisotropy constant K_1 and polarization J_s as a function of x in $HfCo_{7-x}Fe_x$ and $HfCo_7Si_x$ at 300 K.

$HfCo_7$—based alloys as indicated in Fig. 2(b). Note that the law of approach to saturation method yields $K_1 \approx 4.7\ \mathrm{Mergs/cm^3}$ for bulk hcp Co (not shown here), but the magnetization of $HfCo_7$-based alloys is considerably reduced as compared to 1438 $\mathrm{emu/cm^3}$ of bulk hcp Co (not shown in Fig. 2(b)).

K_1 and J_s of $HfCo_{7-x}Fe_x$ and $HfCo_7Si_x$ as a function of x are summarized in Fig. 3. These results show that J_s improves on substituting Fe for Co in $HfCo_{7-x}Fe_x$, but K_1 exhibits a slight decrease for high $x \approx 0.75$ and 1. In the case of $HfCo_7Si_x$, both K_1 and J_s decrease on increasing x. In brief, these results reveal that permanent-magnet properties of $HfCo_7$-based alloys can be tailored by varying the composition of these alloys.

IV. Model Structure and Anisotropy Calculations

Our XRD analysis indicates that $HfCo_7$ has an orthorhombic unit cell with lattice parameters of $a = 4.719$ Å, $b = 4.278$ Å, and $c = 8.070$ Å. Based on these lattice parameters, the metallic radii of dense-packed Hf and Co atoms suggest two formula units in the unit cell, and thus this structure can be realized by an

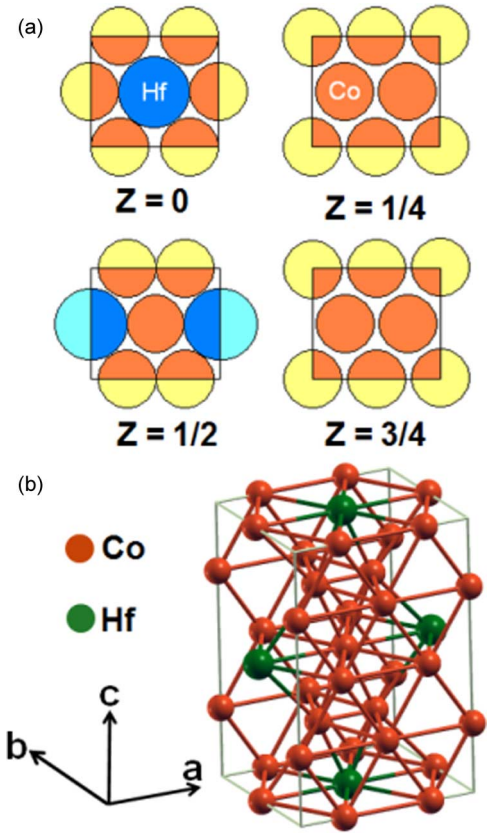

Fig. 4. Structural models for $HfCo_7$, based on experimental lattice parameters: (a) Hard-core model (xy-planes for various z-values) and (b) atomic positions after relaxation using VASP.

atomic hardcore model in which Hf atoms are coordinated with Co atoms as shown in Fig. 4(a). DFT was used to relax the structure inside the unit cell, and Fig. 4(b) shows the corresponding atomic positions in $HfCo_7$. Note that Fig. 4(b) is a model structure aiming at an approximate description of the alloy during quenching, as monitored by XRD. Very likely, the equilibrium structure of $HfCo_7$ is different from Fig. 4(b), with complicated stackings of simple units such as that in Fig. 4(b). Further experimental and theoretical research is necessary to clarify these points.

The structure of Fig. 4(b) is used to calculate the magnetization and the magnetic anisotropy of $HfCo_7$, in the latter case using the energy difference method by including spin-orbital coupling in noncollinear mode [17], [18].

A rather unusual feature of the anisotropy and micromagnetism of orthorhombic crystals is the existence of two lowest-order anisotropy constants, K_1 and K_1', defined by the anisotropy energy [19]

$$\frac{E}{V_{atom}} = K_0 + K_1 \sin^2\theta + K_1' \sin^2\theta \cos 2\varphi \qquad (3)$$

By solving (3) for three principle directions, the following equations are obtained

$$\frac{E_{001}}{V_{cell}} = K_0 \quad (\theta = 0^\circ, \phi = 0^\circ) \qquad (4)$$

$$\frac{E_{100}}{V_{cell}} = K_0 + K_1 + K_1' \quad (\theta = 90^\circ, \phi = 0^\circ) \qquad (5)$$

$$\frac{E_{010}}{V_{cell}} = K_0 + K_1 - K_1' \quad (\theta = 0^\circ, \phi = 90^\circ) \qquad (6)$$

θ and ϕ are the magnetization angles with respect to c and a axes, respectively. The energy values $E_{100} = 0.00$ meV/f.u., $E_{010} = 1.67$ meV/f.u., and $E_{001} = 1.78$ meV/f.u obtained from the DFT calculations make it possible to extract the anisotropy constants from (4)–(6) as $K_1 = -16.46\ \mathrm{Mergs/cm^3}$ and $K_1' = -18.53\ \mathrm{Mergs/cm^3}$, which are in the range of the experimentally measured $K_1 \approx 14.0\ \mathrm{Mergs/cm^3}$ at 300 K for $HfCo_7$. Note that the two anisotropy constants give rise to a small rotational anisotropy (around c), but it is predominantly in-plane. The negative value of K_1 and $K_1'\square$ also suggests that $HfCo_7$ possibly has easy plane anisotropy. However, DFT calculations somewhat overestimate J_s (11.4 kG), as compared to the experimentally room-temperature value of J_s (8.9 kG). This difference can be attributed to the following facts: (i) the theoretical calculations are relevant to zero-temperature and (ii) the experimental magnetization does not saturate even for a field $H \approx 70$ kOe.

In addition, Hf atoms are coupled anti-ferromagnetically with the neighboring Co atoms. The spin and orbital moments of Hf in $HfCo_7$ are -0.32 and $0.011\ \mu\mathrm{B/atom}$, respectively. This coupling reduces the average spin moment of Co in $HfCo_7$ to $1.08\ \mu_\mathrm{B}/\mathrm{atom}$ as compared to $1.6\ \mu\mathrm{B}/\mathrm{atom}$ of bulk Co.

V. Conclusions

In conclusion, $HfCo_7$, $HfCo_{7-x}Fe_x$, and $HfCo_7Si_x$alloys were prepared using melt-spinning method and their structural and magnetic properties were investigated. X-ray diffractions of $HfCo_7$-based alloys were indexed with an orthorhombic structure having lattice parameters of about $a = 4.719$ Å, $b = 4.278$ Å and $c = 8.070$ Å. These studies show that high magnetic anisotropies ($K_1 > 10\ \mathrm{Mergs/cm^3}$) and coercivities ($H_c \approx 3$ kOe) at 300 K can be obtained in $HfCo_7$-based alloys as compared to bulk hcp Co ($K_1 = 4.7\ \mathrm{Mergs/cm^3}$ and $H_c = 0.09$ kOe). In addition, these alloys also exhibit appreciable magnetic polarization in the range of 7.2 to 10.8 kG. This study indicates that $HfCo_7$-based alloys are promising alternative alloys for permanent-magnets, from the view point of mitigating the critical material aspects of rare-earth permanent magnets.

Acknowledgment

This work was supported by the U.S. Department of Energy/BREM (Grant No. DE-AC02-07CH11358, B.D, J.E.S), Advanced Research Projects Agency-Energy (Grant No. DE-AR 0000046, B.B), US Department of Energy (Grant No. DE-FG02-04ER46152, D.J.S.), NSF-Materials Research Science and Engineering Center (Grant No. DMR-0820521, R.S), the Indo-European (PKS, AK), and Nebraska Center for Materials and Nanoscience, V.R.S, X.Z.L.). Thanks are due to P. Manchanda for help in the DFT calculations, and to C.-Z. Wang and K.-M. Ho for helpful discussions regarding the structural determination of $HfCo_7$.

REFERENCES

[1] R. Skomski, J. E. Shield, and D. J. Sellmyer, "An elemental question," Magnetic Technology International, UKIP Media and Events Ltd pp. 26–29, 2011.

[2] N. Jones, "The pull of stronger magnets," *Nature*, vol. 472, pp. 22–23, 2011.

[3] B. Balamurugan, D. J. Sellmyer, G. C. Hadjipanayis, and R. Skomski, "Prospects for nanoparticle-based permanent magnets," *Scripta Mater.*, vol. 67, pp. 542–547, 2012.

[4] K. H. J. Buschow, "Differences in magnetic properties between amorphous and crystalline alloys," *J. Appl. Phys.*, vol. 53, pp. 7713–7116, 1982.

[5] K. H. J. Buschow, "Note on the Hf-Co phase diagram," *J. Less Common Metals*, vol. 59, pp. 61–67, 1978.

[6] Y. Shimada and H. Kojima, "Electron transfer in the Hf_1Co_6 magnetic alloy," *J. Appl. Phys.*, vol. 48, pp. 2626–2227, 1977.

[7] B. G. Demczyk and S. F. Cheng, "Structures of Zr_2Co_{11} and $HfCo_7$ intermetallics forms," *J. Appl. Cryst.*, vol. 24, pp. 1023–1026, 1991.

[8] S. C. Bedi and M. Forker, "Hyperfine interactions at Ta impurities in cobalt and cobalt-hafnium intermetallic compounds," *Phys. Rev. B*, vol. 22, pp. 14948–14960, 1993.

[9] H. Okamoto, *Phase Diagram of Binary Alloys*. Materials Park, OH, USA: ASM, 2000, p. 248.

[10] B. Balamurugan, B. Das, V. R. Shah, R. Skomski, and D. J. Sellmyer, "Assembly of uniaxially aligned rare-earth-free nanomagnets," *Appl. Phys. Lett.*, vol. 101, p. 122407, 2012.

[11] G. Kresse and D. Joubert, "From ultrasoft pseudopotentials to the projector augmented-wave method," *Phys. Rev. B*, vol. 59, pp. 1758–1775, 1999.

[12] P. E. Blöchl, "Projector augmented-wave method," *Phys. Rev. B*, vol. 50, pp. 17953–17979, 1994.

[13] J. P. Perdew, K. Burke, and M. Ernzerhof, "Generalized gradient approximation made simple," *Phys. Rev. Lett.*, vol. 77, pp. 3865–3868, 1996.

[14] G. C. Hadjipanayis, D. J. Sellmyer, and B. Brandt, "Rare-earth-rich metallic glasses. I. Magnetic hysteresis," *Phys. Rev. B*, vol. 23, pp. 3349–3354, 1981.

[15] A. Franco, Jr and F. C. E. Silva, "High temperature magnetic properties of cobalt ferrite nanoparticles," *Appl. Phys. Lett.*, vol. 96, p. 172505, 2010.

[16] E. Kneller, *Ferromagnetism*. Berlin: Springer, 1962.

[17] D. Hobbs, G. Kresse, and J. Hafner, "Fully unconstrained noncollinear magnetism within the projector augmented-wave method," *Phys. Rev. B*, vol. 62, pp. 11556–11560, 2000.

[18] M. Marsman and J. Hafner, "Broken symmetries in the crystalline and magnetic structures of γ-iron," *Phys. Rev. B*, vol. 66, p. 224409, 2002.

[19] R. Skomski and J. M. D. Coey, Permanent Magnetism Institute of Physics. Bristol, 1999.